



Original article

Synthesis and biological evaluation of novel aliphatic amido-quaternary ammonium salts for anticancer chemotherapy: Part II



Jee Sun Yang^a, Doona Song^a, Won Jin Ko^a, Bunyea Kim^a, Bo-Kyung Kim^c, Song-Kyu Park^b, Misun Won^c, Kiho Lee^b, Kyeong Lee^d, Hwan Mook Kim^{e,**}, Gyoonhee Han^{a,f,*}

^a Translational Research Center for Protein Function Control, Department of Biotechnology, Yonsei University, Seoul 120-749, Republic of Korea

^b College of Pharmacy, Korea University, Sejong City 339-700, Republic of Korea

^c Medical Genomics Research Center, KRIBB, Daejeon 305-806, Republic of Korea

^d College of Pharmacy, Dongguk University-Seoul, Seoul 100-715, Republic of Korea

^e College of Pharmacy, Gachon University, Incheon 406-799, Republic of Korea

^f Department of Integrated OMICS for Biomedical Sciences (WCU Program), Yonsei University, Seoul 120-749, Republic of Korea

ARTICLE INFO

Article history:

Received 25 September 2012

Received in revised form

28 December 2012

Accepted 29 December 2012

Available online 14 March 2013

Keywords:

Aliphatic amido-quaternary ammonium salts

Open-ring form of aliphatic amido-quaternary ammonium salts

RhoB

GTPase RA_t Sarcoma (Ras)

Perifosine

NSC126188

ABSTRACT

A series of novel aliphatic amido-quaternary ammonium salts were synthesized and evaluated for their anticancer effects involving induction of RhoB. Most of these compounds, featuring open-ring forms of aliphatic amido-quaternary ammonium salts, exhibited potent anti-proliferative activities in human cancer cell lines, including PC-3, NUGC-3, MDA-MB-231, ACHN, HCT-15, and NCI-H23. In further evaluation, the representative compound *N,N*-diethyl-*N*-(2-(*N*-methyltetradecanamido)ethyl)prop-2-en-1-aminium bromide (**3b**) exhibited potent pro-apoptotic activity, through RhoB activation, in HeLa cells.

© 2013 Elsevier Masson SAS. All rights reserved.

1. Introduction

The Ras genes, the first oncogenes to be identified, are found in approximately 30% of all human cancers: in adenocarcinomas of the pancreas (90%), colon (50%), and lung (30%); in thyroid tumors (50%); and in myeloid leukemia (30%) [1]. The Rho proteins are members of the Ras superfamily. The Rho family itself contains more than 20 members, which regulate diverse cellular functions including cell growth, morphogenesis, cell motility, cytokinesis, cytoskeletal organization, transcriptional activation, and membrane trafficking. They are also essential for Ras transformation, metastasis and apoptosis [2–4].

The Rho family includes RhoA, -B, and -C, Rac1 and -2, and Cdc42. The RhoA-related subgroup contains RhoA, RhoB and RhoC. These three isoforms share ~85% protein sequence identity, with the greatest divergence close to the C-terminus. Despite the high sequence similarity among RhoA-like proteins, they have different activities with respect to cancer: RhoB is a tumor suppressor that promotes growth inhibition and induces apoptosis in cancer cells, whereas RhoA and RhoC promote oncogenesis, invasion, and metastasis [5,6]. Recent studies suggest that RhoB determines the stability and nuclear trafficking of Akt in endothelial cells, where it plays roles in cell survival [7]. Many other reports have demonstrated suppression of RhoB during tumor progression in multiple cancers; consistent with this finding, cancer cell proliferation can be inhibited by restoration of RhoB [8–11]. Therefore, induction of RhoB expression represents a promising target for cancer therapy.

Several studies showed that apoptosis can be induced by activating RhoB protein by treating cells with small-molecule drugs such as farnesyltransferase inhibitors and inhibitors of Akt and PI3K. Ras proteins must be farnesylated in order to exert oncogenic

* Corresponding author. Translational Research Center for Protein Function Control, Department of Biotechnology, Yonsei University, Seoul 120-749, Republic of Korea. Tel.: +82 2 21232882; fax: +82 2 3627265.

** Corresponding author. Tel.: +82 32 8204825; fax: +82 32 8204829.

E-mail addresses: hwanmook@gachon.ac.kr (H.M. Kim), gyoonhee@yonsei.ac.kr, gyoonhee@gmail.com (G. Han).

activity, and RhoB contains farnesyl as well as geranylgeranyl groups [12]. BMS-186511 is a farnesyltransferase inhibitor that inhibits Ras signaling and the transformed growth of spontaneous tumors in H-Ras transgenic mice with minimal toxicity [13]. The protein kinase B (Akt) pathway, which is generally activated in cancer cells, has several downstream targets that regulate tumor-associated cell processes; therefore, blocking this pathway can induce apoptosis and growth inhibition in cancer cells [14]. Furthermore, downregulation of RhoB inhibits transformation, invasion, and metastasis through an Akt-dependent mechanism [15]. Perifosine is a representative Akt inhibitor that targets cellular membranes and is orally bioactive. Furthermore, we have synthesized a series of piperazine alkyl derivatives based on NSC126188, which induces apoptosis through the PI3K/Akt pathway and/or the RhoB mediated pathway [16]. All of these RhoB-induced anticancer agents share common structural features, including a long aliphatic chain (Fig. 1).

Here, we present the synthesis and biological activities of a novel series of aliphatic amido-quaternary ammonium salts, based on our previous study of NSC126188 derivatives. We performed a structure–activity relationship (SAR) study on this series of compounds, based on RhoB activation level and anti-proliferative activities in several human cancer cells. Our results suggest that novel aliphatic amido-quaternary ammonium salts in the open-ring form represent more promising chemotherapeutic anticancer agents than compounds with a piperazine moiety.

2. Chemistry

Based on the amido-piperazinium structures of the compounds described in our previous work, we designed and synthesized 25 analogs with one major modification, namely, introduction of the open-ring form in place of the piperazine moiety. As illustrated in Schemes 1 and 2, the final compounds, **3a–s** and **5a–f**, were synthesized from various fatty acids by two-step procedures based on design. Reactions of the fatty acids **1** with 1-(3-dimethylamino-propyl)-3-ethyl-carbodiimide hydrochloride (EDCI) and 4-dimethylaminopyridine (DMAP) in the presence of dichloromethane resulted in the in situ formation of activated acyl compounds which on further addition of substituted *N*-alkyl diamines, produces the desired amides **2a–j** and **4a–c**, respectively in good yields. Synthesized amides **2** and **4** were converted to desired amido-quaternary ammonium salts **3a–s** and **5a–f** by *N*-alkylation using various alkyl halides in the presence of anhydrous acetonitrile. The structures of amido-quaternary ammonium salts **3** and **5** were confirmed by spectral data. The *N*-alkylation was detected by studying the NMR spectra. The $-\text{CH}_2\text{N}^+(\text{CH}_2)\text{CH}_2-$ protons (δ 3.03–3.94 ppm) are distinctive (downfield) compared to the $-\text{CH}_2\text{N}(\text{CH}_2)\text{CH}_2-$ protons (δ 2.19–2.92 ppm). The ^1H NMR spectra also revealed a triplet signal at δ 0.79–0.91 ppm due to CH_3CH_2- proton. Elemental analyzes were obtained from a Thermo Finnigan model Flash 1112

series EA chemical analyzer. The results of elemental analyzes (C, H, N) were within $\pm 0.4\%$ of the calculated values. All quaternary ammonium salt analogs were characterized and evaluated for *in vitro* biological activities.

3. Results and discussion

All newly synthesized compounds were assayed for growth inhibitory activity in six human cancer cell types: PC-3 (prostate cancer), NUGC-3 (stomach cancer), MDA-MB-231 (breast cancer), ACHN (renal cancer), HCT15 (colon cancer), and NCI-H23 (non-small cell lung cancer). Results are tabulated as GI_{50} values in the micromolar range (Tables 1–4). To evaluate the effect of these compounds on RhoB induction, we conducted RhoB promoter assays. Perifosine and NSC126188 were used as positive references for comparison of *in vitro* activities.

Initially, in order to assess the effects of the open-ring moiety on amido-quaternary ammonium salts, we synthesized 11 compounds (Table 1) based on our previous study. The *N,N*-dimethyl moiety of NSC126188 and the carbon-chain length (14–18 carbons) of the compounds were fixed based on the results of the previous study, and the piperazine ring was replaced with the open-ring form. Multiple *N,N*-dimethyl-diamines, such as *N,N*-dimethylethane-1,2-diamine, *N,N*-dimethylpropane-1,3-diamine, or *N,N,N,N*-tetramethylpropane-1,3-diamine, were introduced at the open-ring position.

The overall activities of the newly synthesized compounds are displayed in Table 1. The compounds significantly inhibited growth, especially in gastric and prostate cancer cell lines. Of note, most of the 11 initially prepared compounds inhibited proliferation in gastric cancer cell lines more effectively than perifosine. Moreover, three analogs, **3a**, **3h**, and **3r**, all synthesized with *N,N*-dimethylethane-1,2-diamine, exhibited remarkably potent growth inhibition than NSC126188 with GI_{50} values of 0.22, 0.17, and 0.13 μM , respectively, in the NUGC-3 cell line. In particular, **3h** also illustrated strong anti-proliferative activity in the PC-3 cell line ($\text{GI}_{50} = 0.37 \mu\text{M}$).

For the synthesis of compounds containing *N,N*-dimethylpropane-1,3-diamine, we used two different reagents, *N,N,N'*-trimethylpropane-1,3-diamine and *N,N*-dimethylpropane-1,3-diamine. Comparisons between **3m** and **3n**, and between **3d** and **3e**, confirm that a methyl group at the *N'* position increases growth inhibitory activity. Furthermore, an *N'*-methyl seems to be important for induction of RhoB expression, as shown in Fig. 2. According to the results of the RhoB promoter assay, all compounds listed in Table 1 induced RhoB expression, although less potently than perifosine in most cases. This result also suggests that the anti-proliferative activities of these compounds are mediated through the RhoB pathway.

We assessed the effect of carbon-chain length on activity, using three groups of compounds classified by *N,N*-dimethyl-diamines with carbon-chains of lengths between 14 and 18 ($n = 12$ –16).

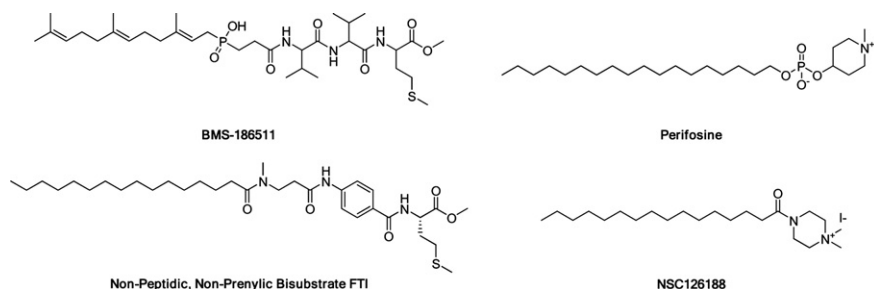
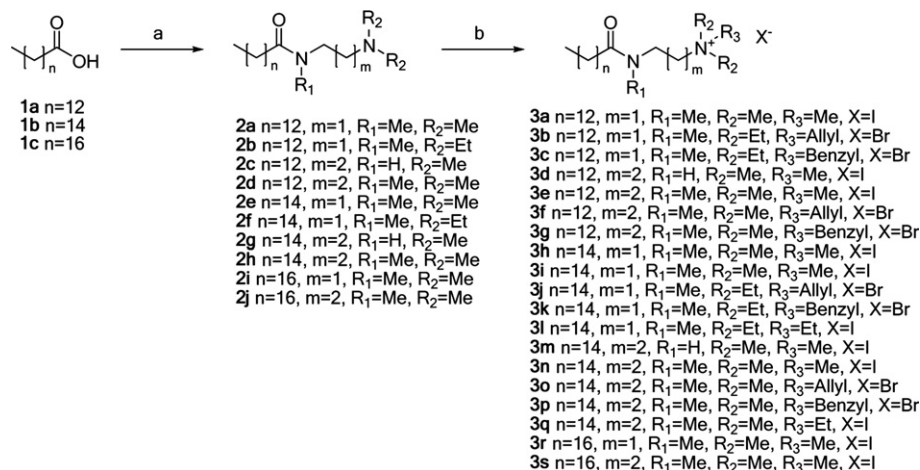


Fig. 1. Chemical structures of farnesyltransferase inhibitors and PI3K/Akt inhibitors.



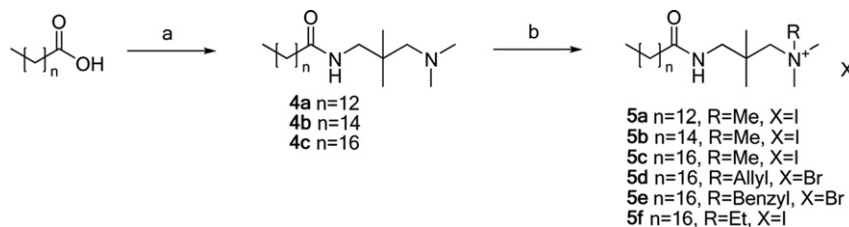
Scheme 1. Reaction protocol for the synthesis of aliphatic amido-quaternary ammonium salts (**3a–s**). Reagents and conditions: (a) DMAP, EDCI, *N,N*-alkyl-diamine, CH_2Cl_2 , overnight; (b) alkyl halide, CH_3CN at $\sim 140\text{--}150^\circ\text{C}$, 7 h.

Among the first group of compounds (*N,N*-dimethylethane-1,2-diamine derivatives, **3a**, **3h**, and **3r**), **3h** ($n = 14$) showed the most striking inhibition of growth in the PC-3 and NUGC-3 cell lines as stated above. Among the second group of compounds synthesized with *N,N,N'*-trimethylpropane-1,3-diamine (**3e**, **3n** and **3s**), **3e** ($n = 12$) displayed the most potent growth inhibition. Of note, whereas the other group of compounds inhibited RhoB expression to a lesser extent than NSC126188 and perifosine, **3n** ($n = 14$) induced RhoB expression to a greater extent than the other compounds in its group. Growth inhibition by compounds containing *N,N,2,2*-tetramethylpropane-1,3-diamine (**5a–c**) was moderate in gastric cancer cell line, with GI_{50} from 0.32 to 0.45 μM . However, **5c**, with a carbon-chain length of 18, exhibited striking activity in a prostate cancer cell line ($\text{GI}_{50} = 0.24 \mu\text{M}$). These results suggest that carbon-chain length is not a major factor in determining anti-proliferative activity, but it might be important in regulating RhoB promoter expression.

Based on compound **3h**, which showed potent anti-proliferative activity in gastric and prostate cancer cell lines and induced the strongest reporter expression in the RhoB promoter-based assay, we prepared six more analogs (Table 2). To evaluate the effect of *N,N*-dialkyl substituents, we synthesized multiple *N,N*-dialkyl substituents using *N,N*-dimethylethane-1,2-diamine. Compounds **3b**, with an allyl group at R_3 , displayed a more robust effect on growth inhibition in the NUGC-3 cell line ($\text{GI}_{50} = 0.14 \mu\text{M}$) and the PC-3 cell line ($\text{GI}_{50} = 0.21 \mu\text{M}$). Other compounds from this series also inhibited the growth of these two cancer cell lines, with GI_{50} under 0.40 μM . Furthermore, the induction of RhoB expression by all of these compounds was far superior to induction by amido-quaternary ammonium salts from other groups. Therefore, we conclude that these compounds inhibit proliferation of cancer cells by upregulating RhoB (Table 2).

In our previous study, **A671** (1-allyl-1-ethyl-4-palmitoylpiperazine-1-ium bromide), which promotes apoptosis through the RhoB pathway, emerged as the most promising chemotherapeutic agent. To evaluate the effect of the open-ring moiety on the activities of amido-quaternary ammonium salts, we compared *N*-ethyl-*N*-allyl substituted compounds (**3b** and **3j**) with **A671**. Except in colon cancer cells, **3b** ($n = 12$) and **3j** ($n = 14$) displayed anti-proliferative activities higher than that of **A671**, which contains a piperazine ring moiety (Table 2). Furthermore, the result of RhoB promoter activation level shows that compounds with the open-ring moiety induced RhoB expression level more than the previously reported compounds (Fig. 2). These results confirm that replacing the piperazine ring with an open-ring diamine is a valid approach to increasing anti-proliferative activity via the RhoB mediated pathway.

Because we had validated that compounds with *N'*-methyl inhibited growth more effectively than compounds with hydrogen at the *N'* position, we retained the *N'*-methyl and fixed carbon-chain length at 14 or 16 in further syntheses. As shown in Table 3, growth inhibition by compounds in this series was not as impressive as inhibition by compounds in Table 2. Most of the compounds in this series displayed equally effective inhibition in the two human cancer cell lines described above. Of interest, compounds with carbon-chain length of 16 (**3o** and **3p**) elevated the expression level of RhoB considerably; however, the RhoB expression level was not proportional to the inhibitory activity of *N,N*-dimethylpropane-1,3-diamine derivatives. Instead, compounds with low RhoB expression exhibited stronger anti-proliferative activity than compounds that induced high levels of RhoB expression. This result indicates that RhoB mediated apoptosis might not represent the main mechanism underlying the efficacies of this series of compounds.



Scheme 2. Reaction protocol for the synthesis of aliphatic amido-quaternary ammonium salts (**5a–f**). Reagents and conditions: (a) DMAP, EDCI, *N,N,2,2*-tetramethylpropane-1,3-diamine, CH_2Cl_2 , overnight; (b) alkyl halide, CH_3CN at $\sim 140\text{--}150^\circ\text{C}$, 7 h.

Table 1
Cell growth-inhibitory activities of compounds substituted with *N,N*-dimethyl-diamine.

Cell line	Tissue	Growth inhibition GI ₅₀ (μM) ^a											NSC126188	Perifosine
		3a	3d	3e	3h	3m	3n	3r	3s	5a	5b	5c		
PC-3	Prostate	0.41	0.39	0.32	0.37	0.60	0.49	0.42	0.52	0.51	0.44	0.24	0.48	0.44
MDA-MB-231	Breast	0.80	1.48	1.78	1.14	2.18	1.42	1.07	2.41	1.31	1.54	1.21	1.44	2.86
ACHN	Kidney	0.26	1.56	1.01	0.45	3.36	0.76	0.36	3.40	3.12	2.60	2.30	1.04	4.56
NUGC-3	Gastric	0.22	0.43	0.32	0.17	1.07	0.19	0.14	0.97	0.84	0.43	0.45	0.29	0.54
HCT15	Colon	1.47	0.79	1.72	1.31	2.56	1.98	0.80	0.79	3.70	NA ^b	1.73	0.58	1.25
NCI-H23	Lung	0.92	1.02	0.56	1.54	2.15	0.96	1.52	1.68	1.44	1.34	1.71	2.34	4.21

^a Growth inhibition was measured by SRB (sulforhodamine B) assay. The values given are means of three experiments.

^b (NA) not active.

Finally, among the compounds containing *N,N,N,N*-tetramethylpropane-1,3-diamine (**5a–c**), compound **5c** was the most potent in prostate cancer cells. Therefore, in subsequent syntheses, only the *N,N*-dialkyl moiety of **5c** was modified (Table 4). Allyl, benzyl, and ethyl groups were introduced at the *N*-position. No compound performed better than **5c**, but the reporter levels in the RhoB promoter-based assay of this series of compounds were moderately good.

Farnesyltransferase inhibitors, perifosine, NSC126188 and amido-quaternary ammonium salts share structural features, including long aliphatic carbon-chains and electronegative atoms (specifically, nitrogen). Furthermore, these compounds control growth inhibition through the RhoB mediated pathway. We have designed and synthesized 25 analogs of novel amido-quaternary ammonium salts with an open-ring form, based on our previous work and the structures of farnesyltransferase inhibitors. The newly synthesized compounds were evaluated for their anticancer effects in six human cancer cell lines. Among them, compound **3b** emerged as the most promising anticancer agent; it was more effective than all other compounds, including the piperazine ring-substituted compounds in our previous study, in terms of potent inhibition of cancer cell growth and stimulation of apoptosis. The effects of **3b** in RhoB promoter-based reporter assays indicate that this compound may act through RhoB mediated signaling. Taken together, the data presented here suggest that novel aliphatic amido-quaternary ammonium salts in the open-ring form represent promising chemotherapeutic anticancer agents that act through the RhoB pathway, and that these compounds are more effective than those containing the piperazine moiety.

4. Experimental section

All chemicals were obtained from commercial suppliers and used without further purification. All reactions were monitored by thin-layer chromatography (TLC) on pre-coated silica gel 60 F₂₅₄ (mesh) (E. Merck, Mumbai, India), and spots were visualized under UV light (254 nm). Flash column chromatography was performed with silica (Merck EM9385, 230–400 mesh). ¹H and ¹³C nuclear magnetic resonance (NMR; Varian) spectra were recorded at 300

and 75 MHz, at 400 and 100 MHz, or at 500 and 125 MHz. Proton and carbon chemical shifts are expressed in ppm relative to internal tetramethylsilane, and coupling constants (*J*) are expressed in Hertz. Liquid chromatography–mass spectrometry (LC/MS) spectra were recorded by electrospray ionization (ESI) on Shimadzu LC/MS instruments (10% 0.1% TFA in H₂O/90% 0.1% TFA in acetonitrile) in scan mode (from 0 to 600 amu/z); the detected ion peaks are (*M*⁺*z*)/*z* and (*M*[−]*z*)/*z* in positive and negative ion modes, respectively, where *M* represents the molecular weight of the compound and *z* represents the charge (number of protons). High resolution mass spectrometry (HRMS) spectra were obtained from electrospray ionization (ESI) – positive mode on the Micromass Q-TOF (Waters Corp., USA; the capillary and sample cone voltages 4000 V & 30 V, the desolvation gas flow 600 L/h at 200 °C, and the source temperature 100 °C) High Resolution Tandem Mass Spectrometer at Yonsei University in Seoul, Korea.

4.1. General procedures for the synthesis of **2a–j** and **4a–c**

Carboxylic acid **1** (2.9 mmol) was dissolved in anhydrous dichloromethane (0.2 M) at room temperature under Argon atmosphere. *N,N*-alkyl-diamine (4.3 mmol), EDC (1-ethyl-3-[3-dimethylaminopropyl]carboimide hydrochloride, 4.3 mmol), and DMAP (4-dimethylaminopyridine, 0.9 mmol) were added, and the mixture was stirred for 8 h at room temperature. Saturated NH₄Cl solution was added, and the mixture was extracted with dichloromethane (3×). The organic layer was washed with brine, dried over anhydrous Na₂SO₄, and concentrated *in vacuo*. The residue was purified by chromatography on silica gel with 5% MeOH/CH₂Cl₂ to afford amides.

4.1.1. *N*-(2-(Dimethylamino)ethyl)-*N*-methyltetradecanamide (**2a**)

¹H NMR (DMSO-*d*₆, 300 MHz) δ 3.36–3.31 (m, 2H), 2.93–2.79 (br m, 3H), 2.37–2.21 (m, 4H), 2.16–2.13 (br m, 6H), 1.46 (br m, 2H), 1.24 (br m, 20H), 0.85 (t, 3H, *J* = 6.3 Hz); ESI-MS: *m/z* = 313 [M⁺H].

4.1.2. *N*-(2-(Diethylamino)ethyl)-*N*-methyltetradecanamide (**2b**)

¹H NMR (CDCl₃, 300 MHz) δ 3.43–3.27 (m, 2H), 2.98–2.89 (m, 3H), 2.56–2.46 (m, 6H), 2.31–2.21 (m, 2H), 1.59–1.55 (m, 2H),

Table 2
Cell growth-inhibitory activities of derivatives of compound **3h**.

Cell line	Tissue	Growth inhibition GI ₅₀ (μM)							A671	NSC126188	perifosine
		3b	3c	3h	3i	3j	3k	3l			
PC-3	Prostate	0.21	0.26	0.37	0.25	0.20	0.31	0.23	0.37	0.48	0.44
MDA-MB-231	Breast	0.30	0.36	1.14	0.66	0.44	1.13	0.36	0.68	1.44	2.86
ACHN	Kidney	0.10	0.23	0.45	0.58	0.35	0.60	0.27	0.50	1.04	4.56
NUGC-3	Gastric	0.14	0.16	0.17	0.41	0.27	0.36	0.16	0.27	0.29	0.54
HCT15	Colon	NA	4.33	1.31	1.01	1.98	NA	0.61	1.33	0.58	1.25
NCI-H23	Lung	0.24	0.28	1.54	0.58	0.17	1.22	1.11	0.88	2.34	4.21

Table 3
Cell growth-inhibitory activities of derivatives of compound **3e**.

Cell line	Tissue	Growth inhibition GI ₅₀ (μM)							
		3e	3f	3g	3o	3p	3q	NSC126188	Perifosine
PC-3	Prostate	0.32	0.31	0.53	0.43	0.85	0.49	0.48	0.44
MDA-MB-231	Breast	1.78	1.35	1.41	0.80	1.35	1.38	1.44	2.86
ACHN	Kidney	1.01	1.89	1.89	0.47	1.30	1.02	1.04	4.56
NUGC-3	Gastric	0.32	0.28	0.43	0.36	0.52	0.22	0.29	0.54
HCT15	Colon	1.72	NA	2.83	NA	NA	3.42	0.58	1.25
NCI-H23	Lung	0.56	0.46	0.66	0.68	1.11	0.78	2.34	4.21

1.24–1.16 (br m, 20H), 1.02–0.94 (m, 6H), 0.85–0.78 (m, 3H); ESI-MS: $m/z = 341$ [M⁺H].

4.1.3. *N*-(3-(Dimethylamino)propyl)tetradecanamide (**2c**)

¹H NMR (CDCl₃, 500 MHz) δ 6.95 (br s, 1H), 3.35 (q, 2H, $J = 5.5$ Hz), 2.50 (t, 2H, $J = 6.5$ Hz), 2.33 (s, 6H), 2.16 (t, 2H, $J = 7.5$ Hz), 1.74–1.71 (m, 2H), 1.61 (br m, 2H), 1.30–1.26 (br m, 20H), 0.88 (t, 3H, $J = 7.0$ Hz); ESI-MS: $m/z = 313$ [M⁺H].

4.1.4. *N*-(3-(Dimethylamino)propyl)-*N*-methyltetradecanamide (**2d**)

¹H NMR (CDCl₃, 500 MHz) δ 3.43–3.32 (m, 2H), 2.96 (ds, 3H, $J = 46.0$ Hz), 2.48 (t, 2H, $J = 7.7$ Hz), 2.39 (s, 3H), 2.35–2.26 (m, 2H), 2.24 (s, 3H), 1.85–1.71 (m, 2H), 1.65–1.61 (m, 2H), 1.30–1.26 (m, 20H), 0.88 (t, 3H, $J = 7.0$ Hz); ESI-MS: $m/z = 327$ [M⁺H].

4.1.5. *N*-(2-(Dimethylamino)ethyl)-*N*-methylpalmitamide (**2e**)

¹H NMR (DMSO-*d*₆, 300 MHz) δ 3.35–3.33 (m, 2H), 2.94–2.79 (br m, 3H), 2.37–2.21 (m, 4H), 2.21–2.13 (br m, 6H), 1.47–1.45 (br m, 2H), 1.24 (br m, 24H), 0.85–0.83 (m, 3H); ESI-MS: $m/z = 341$ [M⁺H].

4.1.6. *N*-(2-(Diethylamino)ethyl)-*N*-methylpalmitamide (**2f**)

¹H NMR (DMSO-*d*₆, 300 MHz) δ 3.29–3.27 (m, 2H), 2.95–2.79 (br m, 3H), 2.49–2.40 (m, 6H), 2.29–2.20 (m, 2H), 1.46 (br m, 2H), 1.24 (br m, 24H), 0.93 (t, 6H, $J = 7.9$ Hz), 0.85 (t, 3H, $J = 6.5$ Hz); ESI-MS: $m/z = 369$ [M⁺H].

4.1.7. *N*-(3-(Dimethylamino)propyl)palmitamide (**2g**)

¹H NMR (DMSO-*d*₆, 400 MHz) δ 8.92 (s, 1H), 3.15–3.08 (m, 2H), 2.31 (t, 2H, $J = 7.2$ Hz), 2.20 (s, 6H), 1.66–1.59 (m, 2H), 1.47–1.45 (m, 2H), 1.20 (s, 26H), 0.81 (t, 3H, $J = 6.6$ Hz); ESI-MS: $m/z = 341$ [M⁺H].

4.1.8. *N*-(3-(Dimethylamino)propyl)-*N*-methylpalmitamide (**2h**)

¹H NMR (DMSO-*d*₆, 400 MHz) δ 3.23 (q, 2H, $J = 8.0$ Hz), 2.25–2.16 (m, 8H), 2.12 (s, 3H), 1.63–1.51 (m, 2H), 1.43 (br s, 2H), 1.20 (s, 26H), 0.81 (t, 3H, $J = 6.8$ Hz); ESI-MS: $m/z = 355$ [M⁺H].

4.1.9. *N*-(2-(Dimethylamino)ethyl)-*N*-methylstearamide (**2i**)

¹H NMR (DMSO-*d*₆, 400 MHz) δ 3.44–3.40 (m, 2H), 2.93–2.79 (ds, 3H), 2.36–2.21 (m, 4H), 2.16 (s, 3H), 2.13 (s, 3H), 1.48–1.39 (m, 2H), 1.23 (m, 28H), 0.85 (t, 3H, $J = 8.0$ Hz); ESI-MS: $m/z = 369$ [M⁺H].

Table 4
Cell growth-inhibitory activities of derivatives of compound **5c**.

Cell line	Tissue	Growth inhibition GI ₅₀ (μM)					
		5c	5d	5e	5f	NSC126188	Perifosine
PC-3	Prostate	0.24	0.47	0.51	0.30	0.48	0.44
MDA-MB-231	Breast	1.21	1.64	2.15	1.12	1.44	2.86
ACHN	Kidney	2.30	1.75	2.23	1.95	1.04	4.56
NUGC-3	Gastric	0.45	0.77	1.32	0.42	0.29	0.54
HCT15	Colon	1.73	NA	NA	2.74	0.58	1.25
NCI-H23	Lung	1.71	0.90	0.91	0.98	2.34	4.21

4.1.10. *N*-(3-(Dimethylamino)propyl)stearamide (**2j**)

¹H NMR (CDCl₃, 500 MHz) δ 7.05 (s, 1H), 3.47–3.33 (m, 2H), 2.81 (t, 2H, $J = 7.2$ Hz), 2.62 (s, 6H), 2.21 (t, 2H, $J = 7.3$ Hz), 1.95 (s, 2H), 1.62 (s, 2H), 1.27 (d, 28H, $J = 17.3$ Hz), 0.89 (t, 3H, $J = 6.8$ Hz); ESI-MS: $m/z = 369$ [M⁺H].

4.1.11. *N*-(3-(Dimethylamino)-2,2-dimethylpropyl)tetradecanamide (**4a**)

¹H NMR (DMSO-*d*₆, 500 MHz) δ 7.57 (t, 1H, $J = 5.7$ Hz), 2.92 (d, 2H, $J = 6.0$ Hz), 2.20 (s, 6H), 2.08 (t, 2H, $J = 7.3$ Hz), 2.04 (s, 2H), 1.48–1.46 (m, 2H), 1.27–1.23 (m, 20H), 0.85 (t, 3H, $J = 6.8$ Hz), 0.78 (s, 6H); ESI-MS: $m/z = 341$ [M⁺H].

4.1.12. *N*-(3-(Dimethylamino)-2,2-dimethylpropyl)palmitamide (**4b**)

¹H NMR (DMSO-*d*₆, 400 MHz) δ 7.56 (s, 1H), 2.91 (d, 2H, $J = 4.8$ Hz), 2.19 (s, 6H), 2.08–2.03 (m, 4H), 1.47–1.46 (m, 2H), 1.22 (s, 24H), 0.84 (t, 3H, $J = 5.4$ Hz), 0.77 (s, 6H); ESI-MS: $m/z = 369$ [M⁺H].

4.1.13. *N*-(3-(Dimethylamino)-2,2-dimethylpropyl)stearamide (**4c**)

¹H NMR (CDCl₃, 500 MHz) δ 7.27 (d, 1H, $J = 2.2$ Hz), 3.26 (s, 2H), 2.87–2.43 (m, 8H), 2.26 (s, 2H), 1.62 (d, 2H, $J = 7.2$ Hz), 1.34–1.20 (m, 28H), 1.18–1.01 (m, 6H), 0.87 (t, 4H, $J = 7.0$ Hz); ESI-MS: $m/z = 397$ [M⁺H].

4.2. General procedures for the synthesis of **3a–s** and **5a–f**

Alkyl halide (1.6 mmol) was added to a solution of **2a–j** and **4a–c** (0.8 mmol) in anhydrous acetonitrile (0.3 M) at room temperature, and the reaction mixture was heated to ~140–150 °C for 7 h. After the reaction mixture equilibrated to room temperature, the precipitate was granulated for 1 h at 0 °C. Solids were collected by filtration, washed with ethyl acetate, and dried *in vacuo*.

4.2.1. *N,N,N*-Trimethyl-2-(*N*-methyltetradecanamido)ethanaminium iodide (**3a**)

¹H NMR (DMSO-*d*₆, 300 MHz) δ 3.71–3.66 (m, 2H), 3.42–3.38 (m, 2H), 3.08 (br, 9H), 3.00 (s, 3H), 2.29 (t, 2H, $J = 7.4$ Hz), 1.47 (br m, 2H), 1.24 (br s, 20H), 0.85 (t, 3H, $J = 6.9$ Hz); ¹³C NMR (DMSO-*d*₆, 100 MHz) δ 172.89 and 171.99, 61.24 and 60.99, 54.40 and 52.43, 54.36 and 52.40, 54.32 and 52.36, 42.36 and 41.11, 35.19, 33.22 and 32.44, 31.68 and 31.32, 29.10, 29.09, 29.07, 29.05, 29.03, 28.97, 28.81, 28.77, 28.75, 24.75 and 24.40, 22.13, 13.98 ppm; ESI-MS: $m/z = 327$ [M⁺]; HRMS (ESI) calcd. for C₂₀H₄₃N₂O (M⁺) 327.3375, found 327.3387.

4.2.2. *N,N*-Diethyl-*N*-(2-(*N*-methyltetradecanamido)ethyl)prop-2-en-1-aminium bromide (**3b**)

¹H NMR (DMSO-*d*₆, 300 MHz) δ 6.09–6.00 (m, 1H), 5.72–5.61 (m, 2H), 4.04–4.01 (m, 2H), 3.94–3.91 (m, 2H), 3.63 (m, 2H), 3.29–3.19 (m, 4H), 3.01 (s, 3H), 2.29 (t, 2H, $J = 7.7$ Hz), 1.47 (m, 2H), 1.27–1.15 (m, 26H), 0.87–0.83 (m, 3H); ¹³C NMR (DMSO-*d*₆, 100 MHz) δ 172.91 and 171.97, 127.21 and 126.80, 125.74 and 125.55,

(DMSO-*d*₆, 100 MHz) δ 172.91 and 171.96, 127.22 and 126.81, 125.76 and 125.54, 59.43, 53.30 and 53.19 (2), 52.43, 40.64, 35.72, 32.70 and 32.37, 31.66 and 31.34, 29.11 (3), 29.07, 29.05, 28.99, 28.83, 28.78 (2), 28.77, 24.72 and 24.42, 22.14, 13.98, 7.49 and 7.27 (2) ppm; ESI-MS: $m/z = 410$ [M^+]; HRMS (ESI) calcd. for C₂₆H₅₃N₂O (M^+) 409.4158, found 409.4151; EA for C₂₆H₅₃N₂OBr calculated: C, 63.78; H, 10.91; N, 5.72; found: C, 63.80; H, 11.20; N, 5.50.

4.2.11. *N*-Benzyl-*N,N*-diethyl-2-(*N*-methylpalmitamido)ethanaminium bromide (**3k**)

¹H NMR (DMSO-*d*₆, 300 MHz) δ 7.53 (s, 5H), 4.64 (s, 2H), 4.00–3.67 (m, 2H), 3.61–3.50 (m, 2H), 3.50–3.32 (m, 4H), 2.98 (s, 3H), 2.32–2.24 (m, 2H), 2.24–2.15 (m, 2H), 1.52–1.43 (m, 2H), 1.32–1.21 (m, 28H), 0.85 (t, 3H, $J = 6.9$ Hz); ¹³C NMR (DMSO-*d*₆, 100 MHz) δ 172.15 and 171.90, 133.33 and 133.28 (2), 130.27, 128.90 (2), 127.97 and 127.95, 67.02 and 66.89, 63.43 and 63.37, 62.10 and 61.59, 47.30 and 47.18, 45.11 and 42.80, 36.82, 32.70 and 32.59, 31.34, 29.11 (3), 29.06 (2), 29.01, 28.85 (2), 28.76, 24.72 and 24.52, 22.14, 21.43, 20.77, 13.99 ppm; ESI-MS: $m/z = 459$ [M^+].

4.2.12. *N,N,N*-Triethyl-2-(*N*-methylpalmitamido)ethanaminium iodide (**3l**)

¹H NMR (DMSO-*d*₆, 300 MHz) δ 3.61–3.56 (m, 2H), 3.33–3.17 (m, 8H), 3.01–2.84 (d, 3H), 3.31–2.26 (t, 2H, $J = 7.3$ Hz), 1.47 (br m, 2H), 1.24–1.19 (br m, 33H), 0.87–0.83 (t, 3H, $J = 6.6$ Hz); ¹³C NMR (DMSO-*d*₆, 100 MHz) δ 172.88 and 171.93, 52.58 and 52.45 (3), 51.86, 40.60, 35.76, 33.33 and 32.38, 31.61 and 31.33, 29.10 (3), 29.05, 29.03 (2), 28.98, 28.83, 28.77, 28.75, 24.69 and 24.41, 22.13, 13.98, 7.41 and 7.20 (3) ppm; ESI-MS: $m/z = 397$ [M^+]; HRMS (ESI) calcd. for C₂₅H₅₃N₂O (M^+) 397.4158, found 397.4153; EA for C₂₅H₅₃N₂OI calculated: C, 57.24; H, 10.18; N, 5.34; found: C, 57.34; H, 10.12; N, 5.24.

4.2.13. *N,N,N*-Trimethyl-3-palmitamidopropan-1-aminium iodide (**3m**)

¹H NMR (DMSO-*d*₆, 500 MHz) δ 8.12–8.11 (d, 1H, $J = 7.5$ Hz), 3.41–3.38 (m, 2H), 3.30 (t, 2H, $J = 7.2$ Hz), 3.27 (s, 2H), 3.16 (s, 9H), 2.23 (t, 2H, $J = 7.5$ Hz), 2.03–1.99 (m, 2H), 1.64–1.61 (m, 2H), 1.34–1.30 (m, 24H), 0.91 (t, 3H, $J = 6.8$ Hz); ESI-MS: $m/z = 355$ [M^+]; HRMS (ESI) calcd. for C₂₂H₄₇N₂O (M^+) 355.3688, found 355.3691.

4.2.14. *N,N,N*-Trimethyl-3-(*N*-methylpalmitamido)propan-1-aminium iodide (**3n**)

¹H NMR (DMSO-*d*₆, 500 MHz) δ 3.33–3.28 (m, 3H), 3.22 (t, 2H, $J = 8.2$ Hz), 3.06 (s, 3H), 3.04 (s, 6H), 2.96 (s, 2H), 2.27 (t, 2H, $J = 7.2$ Hz), 1.89–1.85 (m, 2H), 1.47 (m, 2H), 1.24 (m, 24H), 0.85 (t, 3H, $J = 6.5$ Hz); ESI-MS: $m/z = 370$ [M^+]; HRMS (ESI) calcd. for C₂₃H₄₉N₂O (M^+) 369.3845, found 369.3849.

4.2.15. *N,N*-Dimethyl-*N*-(3-(*N*-methylpalmitamido)propyl)prop-2-en-1-aminium bromide (**3o**)

¹H NMR (DMSO-*d*₆, 500 MHz) δ 6.02–5.90 (m, 1H), 5.57–5.53 (m, 2H), 3.91–3.85 (m, 2H), 3.33–3.22 (m, 5H), 3.13–3.08 (m, 2H), 2.93–2.89 (m, 8H), 2.22–2.18 (m, 2H), 1.92–1.78 (m, 2H), 1.40–1.32 (m, 2H), 1.19–1.00 (m, 24H), 0.79 (t, 3H, $J = 8.5$ Hz); ESI-MS: $m/z = 395$ [M^+]; HRMS (ESI) calcd. for C₂₅H₅₁N₂O (M^+) 395.4001, found 395.3984.

4.2.16. *N*-Benzyl-*N,N*-dimethyl-3-(*N*-methylpalmitamido)propan-1-aminium bromide (**3p**)

¹H NMR (DMSO-*d*₆, 500 MHz) δ 3.34–3.33 (m, 5H), 3.18 (t, 2H, $J = 8.0$ Hz), 2.98–2.95 (m, 8H), 2.26 (t, 2H, $J = 7.5$ Hz), 2.00–1.97 (m, 2H), 1.47–1.46 (m, 2H), 1.23 (m, 24H), 0.85 (t, 3H, $J = 6.5$ Hz); ESI-MS: $m/z = 445$ [M^+]; HRMS (ESI) calcd. for C₂₉H₅₃N₂O (M^+) 445.4158, found 445.4144.

4.2.17. *N*-Ethyl-*N,N*-dimethyl-3-(*N*-methylpalmitamido)propan-1-aminium iodide (**3q**)

¹H NMR (DMSO-*d*₆, 500 MHz) δ 3.36–3.27 (m, 5H), 3.17–3.13 (m, 2H), 2.97–2.93 (m, 8H), 2.29–2.24 (m, 2H), 1.91–1.79 (m, 2H), 1.46–1.34 (m, 2H), 1.22–1.09 (m, 2H), 0.84 (t, 3H, $J = 8.5$ Hz); ESI-MS: $m/z = 383$ [M^+]; HRMS (ESI) calcd. for C₂₄H₅₁N₂O (M^+) 383.4001, found 383.4005.

4.2.18. *N,N,N*-Trimethyl-2-(*N*-methylstearamido)ethanaminium iodide (**3r**)

¹H NMR (DMSO-*d*₆, 500 MHz) δ 3.69 (t, 2H, $J = 7.3$ Hz), 3.41 (t, 2H, $J = 7.3$ Hz), 3.10–3.09 (m, 9H), 3.00 (s, 3H), 2.31–2.28 (m, 2H), 1.48–1.45 (m, 2H), 1.23–1.19 (m, 28H), 0.85 (t, 3H, $J = 7.0$ Hz); ¹³C NMR (DMSO-*d*₆, 100 MHz) δ 172.89 and 171.98, 61.24 and 61.00, 52.44, 52.40, 52.37, 42.36 and 41.12, 35.17, 33.21 and 32.45, 31.68 and 31.34, 29.10 (5), 29.06, 29.00 (2), 28.84, 28.80 (2), 28.76, 24.76 and 24.42, 22.14, 13.98 ppm; ESI-MS: $m/z = 383$ [M^+]; HRMS (ESI) calcd. for C₂₄H₅₁N₂O (M^+) 383.4001, found 383.4017.

4.2.19. *N,N,N*-Trimethyl-3-stearamidopropan-1-aminium iodide (**3s**)

¹H NMR (DMSO-*d*₆, 500 MHz) δ 7.88–7.87 (m, 1H), 3.27–3.23 (m, 2H), 3.11–3.07 (m, 2H), 3.03 (s, 9H), 2.05 (t, 3H, $J = 7.5$ Hz), 1.83–1.77 (m, 2H), 1.49–1.46 (m, 2H), 1.27–1.23 (br m, 28H), 0.85 (t, 3H, $J = 7.0$ Hz); ¹³C NMR (DMSO-*d*₆, 100 MHz) δ 172.32, 63.50, 52.27, 52.24, 52.20, 35.45, 31.33, 29.10 (3), 29.05 (2), 29.01 (2), 28.89 (2), 28.80 (2), 28.76 (2), 25.21, 23.02, 22.14, 13.99 ppm; ESI-MS: $m/z = 383$ [M^+]; HRMS (ESI) calcd. for C₂₄H₅₁N₂O (M^+) 383.4001, found 383.4001.

4.2.20. *N,N,N,2,2*-Pentamethyl-3-tetradecanamidopropan-1-aminium iodide (**5a**)

¹H NMR (DMSO-*d*₆, 500 MHz) δ 7.85 (t, 1H, $J = 6.3$ Hz), 3.26 (s, 2H), 3.17 (s, 9H), 3.05 (d, 2H, $J = 6.5$ Hz), 2.13 (t, 2H, $J = 7.5$ Hz), 1.50 (m, 2H), 1.24 (br m, 20H), 1.07 (s, 6H), 0.85 (t, 3H, $J = 6.8$ Hz); ¹³C NMR (DMSO-*d*₆, 100 MHz) δ 172.89, 72.55, 54.78 (3), 48.00, 37.23, 35.39, 31.33, 29.11 (2), 29.07, 29.06 (2), 29.01, 28.82, 28.76 (2), 25.33, 24.60, 22.14, 14.00 ppm; ESI-MS: $m/z = 355$ [M^+]; HRMS (ESI) calcd. for C₂₂H₄₇N₂O (M^+) 355.3688, found 355.3689.

4.2.21. *N*-Ethyl-*N,N,2,2*-tetramethyl-3-palmitamidopropan-1-aminium iodide (**5b**)

¹H NMR (DMSO-*d*₆, 500 MHz) δ 7.83 (t, NH, $J = 6.0$ Hz), 3.24 (s, 2H), 3.15 (br s, 8H), 3.05 (d, 2H, $J = 6.4$ Hz), 2.13 (t, 2H, $J = 7.4$ Hz), 1.51–1.48 (m, 2H), 1.23 (br m, 27H), 1.07 (s, 6H), 0.85 (t, 3H, $J = 6.6$ Hz); ESI-MS: $m/z = 397$ [M^+].

4.2.22. *N,N,N,2,2*-Pentamethyl-3-stearamidopropan-1-aminium iodide (**5c**)

¹H NMR (DMSO-*d*₆, 500 MHz) δ 7.84 (t, 1H, $J = 6.4$ Hz), 3.30 (s, 9H), 3.23 (s, 2H), 3.14 (s, 2H), 2.12 (t, 2H, $J = 7.4$ Hz), 1.52–1.46 (m, 2H), 1.23 (s, 28H), 1.07 (s, 6H), 0.85 (t, 3H, $J = 6.9$ Hz); ESI-MS: $m/z = 411$ [M^+]; HRMS (ESI) calcd. for C₂₆H₅₅N₂O (M^+) 411.4314, found 411.4318; EA for C₂₆H₅₅N₂OI calculated: C, 57.98; H, 10.29; N, 5.20; found: C, 57.97; H, 10.16; N, 5.09.

4.2.23. *N*-(2,2-Dimethyl-3-stearamidopropyl)-*N,N*-dimethylprop-2-en-1-aminium bromide (**5d**)

¹H NMR (DMSO-*d*₆, 500 MHz) δ 7.85 (s, 1H), 6.07–6.01 (m, 1H), 5.64–5.60 (m, 2H), 4.00 (d, 2H, $J = 7.5$ Hz), 3.17 (s, 2H), 3.04 (d, 2H, $J = 6.0$ Hz), 2.13 (t, 2H, $J = 7.5$ Hz), 1.51–1.50 (m, 2H), 1.27–1.19 (m, 28H), 1.10 (s, 6H), 0.85 (t, 3H, $J = 7.0$ Hz); ¹³C NMR (DMSO-*d*₆, 100 MHz) δ 172.93, 127.68, 126.24, 70.22, 68.75, 51.33, 48.33, 46.16 and 45.71, 37.24, 35.38, 31.36, 29.12 (3), 29.08 (2), 29.06, 28.90 (2), 28.85, 28.81, 28.78 (2), 25.41, 24.84, 23.77 and 22.15 (2), 13.98 ppm; ESI-MS: $m/z = 437$ [M^+]; HRMS (ESI) calcd. for C₂₈H₅₇N₂O (M^+) 437.4471, found 437.4451.

4.2.24. *N*-Benzyl-*N,N*,2,2-tetramethyl-3-stearamidopropan-1-aminium bromide (**5e**)

¹H NMR (DMSO-*d*₆, 500 MHz) δ 7.85 (s, 1H), 7.58–7.47 (m, 5H), 4.56 (s, 2H), 3.31 (s, 6H), 3.27 (d, 2H, *J* = 4.2 Hz), 3.06 (d, 2H, *J* = 9.5 Hz), 2.08 (dd, 2H, *J* = 13.2, 5.7 Hz), 1.47 (d, 2H, *J* = 7.0 Hz), 1.22 (s, 28H), 1.13 (s, 6H), 0.84 (t, 3H, *J* = 6.9 Hz); ¹³C NMR (DMSO-*d*₆, 100 MHz) δ 172.90, 133.29 (2), 130.28, 128.83 (2), 128.18, 71.20, 69.97, 50.73 (2), 48.68, 37.27, 35.36, 31.34, 29.09 (5), 29.02, 28.85 (2), 28.79 (2), 28.76 (2), 25.32, 25.02, 23.80, 22.15, 14.02 ppm; ESI-MS: *m/z* = 487 [M⁺]; HRMS (ESI) calcd. for C₃₂H₅₉N₂O (M⁺) 487.4627, found 487.4622.

4.2.25. *N*-Ethyl-*N,N*,2,2-tetramethyl-3-stearamidopropan-1-aminium iodide (**5f**)

¹H NMR (DMSO-*d*₆, 500 MHz) δ 7.85 (dd, 1H, *J* = 14.2, 7.9 Hz), 3.35–3.27 (m, 8H), 3.14 (s, 2H), 3.07 (s, 2H), 2.12 (t, 2H, *J* = 7.4 Hz), 1.51 (s, 2H), 1.28–1.19 (m, 31H), 1.08 (s, 6H), 0.85 (t, 3H, *J* = 7.0 Hz); ¹³C NMR (DMSO-*d*₆, 100 MHz) δ 172.91, 72.55, 69.71, 62.31, 54.78, 51.27, 48.45 and 48.00, 37.20, 35.39, 31.33, 29.09 (5), 29.05, 29.03, 28.85, 28.78, 28.76 (2), 25.36 and 25.34, 24.69 and 24.60, 22.14, 13.98, 8.24 ppm; ESI-MS: *m/z* = 425 [M⁺]; HRMS (ESI) calcd. for C₂₇H₅₇N₂O (M⁺) 425.4471, found 425.4477.

4.3. Sulforhodamine B (SRB) assay

Growth inhibition of cancer cell lines in the presence of NSC126188 and perifosine was determined using the SRB assay, as previously described [17]. SRB dye bound to the cell matrix was quantified using a spectrophotometer at 530 nm.

4.4. Luciferase assay

Transactivation of RhoB was determined by reporter assay using the dual-luciferase reporter assay system (Promega, Madison, WI, USA), as previously described [18]. HeLa cells at 75–90% confluence were transiently cotransfected with a plasmid encoding pGL2-RhoB-firefly luciferase under control of the RhoB promoter and pRL-SV40-*Renilla* luciferase. Luciferase activity was integrated over a 10-s period and measured using a luminometer (Victor X Light; Perkin Elmer, Waltham, MA, USA). The results were normalized to the levels of *Renilla* luciferase.

Acknowledgments

This research was supported by National Research Foundation (2012-0000884); Korean Research WCU grant (R31-2008-000-10086-0); and the Brain Korea 21 Project of the Republic of Korea.

Appendix A. Supplementary data

Supplementary data related to this article can be found at <http://dx.doi.org/10.1016/j.ejmech.2012.12.063>.

References

- [1] J.L. Bos, Ras oncogenes in human cancer: a review, *Cancer Res.* 49 (1989) 4682–4689.
- [2] J. Chant, L. Stowers, GTPase cascades choreographing cellular behavior: movement, morphogenesis, and more, *Cell* 81 (1995) 1–4.
- [3] R. Khosravi-Far, P.A. Solski, G.J. Clark, M.S. Kinch, C.J. Der, Activation of Rac1, RhoA, and mitogen-activated protein kinases is required for Ras transformation, *Mol. Cell Biol.* 15 (1995) 6443–6453.
- [4] R.G. Qiu, J. Chen, D. Kirn, F. McCormick, M. Symons, An essential role for Rac in Ras transformation, *Nature* 374 (1995) 457–459.
- [5] D.M. Kim, K.S. Chung, S.J. Choi, Y.J. Jung, S.K. Park, G.H. Han, J.S. Ha, K.B. Song, N.S. Choi, H.M. Kim, M. Won, Y.S. Seo, RhoB induces apoptosis via direct interaction with TNFAIP1 in HeLa cells, *Int. J. Cancer* 125 (2009) 2520–2527.
- [6] G.C. Prendergast, Actin' up: RhoB in cancer and apoptosis, *Nat. Rev. Cancer* 1 (2001) 162–168.
- [7] I. Adini, I. Rabinovitz, J.F. Sun, G.C. Prendergast, L.E. Benjamin, RhoB controls Akt trafficking and stage-specific survival of endothelial cells during vascular development, *Genes Dev.* 17 (2003) 2721–2732.
- [8] L.A. Marlow, L.A. Reynolds, A.S. Cleland, S.J. Cooper, M.L. Gumz, S. Kurakata, K. Fujiwara, Y. Zhang, T. Sebo, C. Grant, B. McIver, J.T. Wadsworth, D.C. Radisky, R.C. Smallridge, J.A. Copland, Reactivation of suppressed RhoB is a critical step for the inhibition of anaplastic thyroid cancer growth, *Cancer Res.* 69 (2009) 1536–1544.
- [9] J. Mazieres, T. Antonia, G. Daste, C. Muro-Cacho, D. Berchery, V. Tillement, A. Pradines, S. Sebti, G. Favre, Loss of RhoB expression in human lung cancer progression, *Clin. Cancer Res.* 10 (2004) 2742–2750.
- [10] B. Couderc, A. Pradines, A. Rafii, M. Golzio, A. Deviers, C. Allal, D. Berg, M. Penary, J. Teissie, G. Favre, In vivo restoration of RhoB expression leads to ovarian tumor regression, *Cancer Gene Ther.* 15 (2008) 456–464.
- [11] S. Wang, Y. Yan-Neale, D. Fischer, M. Zeremski, R. Cai, J. Zhu, F. Asselbergs, G. Hampton, D. Cohen, Histone deacetylase 1 represses the small GTPase RhoB expression in human nonsmall lung carcinoma cell line, *Oncogene* 22 (2003) 6204–6213.
- [12] P. Adamson, C.J. Marshall, A. Hall, P.A. Tilbrook, Post-translational modifications of p21^{rho} proteins, *J. Biol. Chem.* 267 (1992) 20033–20038.
- [13] V. Manne, N. Yan, J.M. Carboni, A.V. Tuomari, C.S. Ricca, J.G. Brown, M.L. Andahazy, R.J. Schmidt, D. Patel, R. Zahler, et al., Bisubstrate inhibitors of farnesyltransferase: a novel class of specific inhibitors of ras transformed cells, *Oncogene* 10 (1995) 1763–1779.
- [14] C.W. Lindsley, The Akt/PKB family of protein kinases: a review of small molecule inhibitors and progress towards target validation: a 2009 update, *Curr. Top. Med. Chem.* 10 (2010) 458–477.
- [15] K. Jiang, J. Sun, J. Cheng, J.Y. Djeu, S. Wei, S. Sebti, Akt mediates Ras down-regulation of RhoB, a suppressor of transformation, invasion, and metastasis, *Mol. Cell Biol.* 24 (2004) 5565–5576.
- [16] J.S. Yang, D. Song, B. Lee, W.J. Ko, S.K. Park, M. Won, K. Lee, H.M. Kim, G. Han, Synthesis and biological evaluation of novel aliphatic amido-quaternary ammonium salts for anticancer chemotherapy: part I, *Eur. J. Med. Chem.* 46 (2011) 2861–2866.
- [17] D.M. Kim, S.Y. Koo, K. Jeon, M.H. Kim, J. Lee, C.Y. Hong, S. Jeong, Rapid induction of apoptosis by combination of flavopiridol and tumor necrosis factor (TNF)-alpha or TNF-related apoptosis-inducing ligand in human cancer cell lines, *Cancer Res.* 63 (2003) 621–626.
- [18] M.S. Won, N. Im, S. Park, S.K. Boovanahalli, Y. Jin, X. Jin, K.S. Chung, M. Kang, K. Lee, S.K. Park, H.M. Kim, B.M. Kwon, J.J. Lee, A novel benzimidazole analogue inhibits the hypoxia-inducible factor (HIF)-1 pathway, *Biochem. Biophys. Res. Commun.* 385 (2009) 16–21.